Limnol. Oceanogr., 54(5), 2009, 1425–1437

Coastal oceanographic processes influence the growth and size of a key estuarine species, the Olympia oyster

David L. Kimbro,[a,b,1,*] John Largier,[a,b] and Edwin D. Grosholz[a]

[a] University of California at Davis, Environmental Science and Policy, Davis, California
[b] Bodega Marine Laboratory, Bodega Bay, California

Abstract

Here we empirically demonstrate that a tidal exchange gradient in a central California estuary leads to inversely related spatial gradients in upwelled nutrients and water residence times. As a result, seasonal phytoplankton blooms (summer–fall) occur in the middle of the bay, where nutrient levels and water residence times are intermediate, while seasonal temperature maximums occur in the inner bay, where water residence times are highest and nutrient levels are lowest. By experimentally out-planting juvenile Olympia oysters (*Ostrea lurida*) throughout the estuary, we found that the growth and size of juvenile oysters are better explained by the spatial pattern of phytoplankton concentrations than by that of water temperature. Furthermore, this benthic–pelagic link helps explain the distribution of adult oyster sizes throughout the estuary. Because a phytoplankton maximum can be maintained by a physical interaction between intensive upwelling and a seasonal low-inflow estuary, benthic invertebrates within protected embayments of upwelling regions may not conform to the regional generalization that their growth and size are negatively correlated with upwelling intensity.

Understanding how nearshore oceanography affects benthic population and community dynamics remains one of the outstanding challenges for marine ecology, despite a growing number of studies that link the two (Menge 1992; Leslie et al. 2005; Blanchette et al. 2007). For example, when upwelling occurs in eastern boundary current regions of ocean basins, alongshore winds create an offshore Ekman Transport of nearshore surface waters that in turn brings nutrient-rich and cold subsurface waters up and into the euphotic zone (Mann and Lazier 2006). On the one hand, by elevating nutrient concentrations in the clear, light-filled surface waters, upwelling can increase primary production rates and phytoplankton biomass and consequently enhance the growth of benthic suspension-feeding invertebrates along rocky intertidal shorelines (Menge et al. 1997, 2003; Dugdale et al. 2006). On the other hand, by reducing the temperature of surface waters, upwelling can also slow invertebrate food intake, assimilation, and, therefore, growth (Sanford and Menge 2001). Because upwelling increases nutrients but reduces water temperature, the relationship between upwelling and the growth of benthic invertebrates (e.g., mussels) is complex and may not be amenable to generalization.

While the effect of coastal upwelling on benthic invertebrates through temperature is straightforward, upwelling's effect on invertebrate growth through nutrients and phytoplankton may depend on the intensity of upwelling (Dugdale et al. 2006; Largier et al. 2006; Blanchette et al. 2007). Nearshore phytoplankton blooms require that the rate of photosynthesis sufficiently exceeds the rate of respiration so that phytoplankton will accumulate, despite being diluted by mixing forces (Mann and Lazier 2006). If the wind-driven upwelling that delivers nutrients is intense, it will dilute phytoplankton concentrations by rapidly mixing waters to depth and transporting phytoplankton-rich waters offshore (Largier et al. 2006). Accordingly, intense upwelling will slow invertebrate growth by exposing benthic invertebrates to low levels of food and cold water. In contrast, the alongshore winds in non-upwelling and intermittent-upwelling regions may accelerate invertebrate growth, because the former will expose invertebrates to low levels of food but warm water that may increase feeding and assimilation rates, while the latter may briefly expose invertebrates to both phytoplankton blooms and warm temperatures when upwelling winds relax (Wing et al. 1995; Blanchette et al. 2007; Menge et al. 2008). Given these circumstances, some researchers have generalized that the growth rate and size of benthic invertebrates are greater along coastlines in non- and intermittent-upwelling regions than in intense upwelling regions (Blanchette et al. 2007).

Physical features along coastlines, however, may undermine such a generalization by allowing intensive upwelling to positively affect invertebrate growth. For instance, in upwelling shadows (areas of weak or zero upwelling downwind of headlands), high-nutrient waters that upwell at the headland are advected into adjacent bays (Graham and Largier 1997). There, weak mixing forces enable the upwelled waters to warm and to accumulate phytoplankton, and high densities of phytoplankton persist as long as the upwelling continues (Graham and Largier 1997; Pitcher and Nelson 2006; Vander Woude et al. 2006). Therefore, upwelling shadows are a predictable habitat of phytoplankton-rich and warm waters within an intensive upwelling region. In upwelling shadows, warm temperatures and abundant phytoplankton may both enhance the growth and size of benthic invertebrates (Graham and Largier 1997; Broitman and Kinlan 2006; Pinones et al. 2007).

Coastlines of upwelling regions possess another, yet under-appreciated, physical feature that may cause intense upwelling to increase the growth of benthic invertebrates.

* Corresponding author: dkimbro@bio.fsu.edu

[1] Present address: Florida State University Coastal and Marine Laboratory, St. Teresa, Florida

In upwelling regions with Mediterranean climates (i.e., distinct wet and dry seasons), such as northern California, the inner portions of semi-enclosed bays receive little freshwater input and experience high evaporation during summer and autumn, when nearshore upwelling is intense (Fig. 1A) (Mann and Lazier 2006). During this low-inflow estuarine (LIE) season (Largier et al. 1996) these estuaries lack a classical longitudinal salinity gradient and estuarine circulation, such that the retention times of water (i.e., mixing rates) and the supply of coastally upwelled nutrients within the estuary depend solely on the daily pumping of water with each high and low tide (Largier et al. 1997). Because the horizontal distance that water is pumped—the tidal excursion—decreases with distance from the mouth of a typical LIE, mixing rates decrease as well; a concomitant increase in residence times of water may seasonally yield spatially predictable phytoplankton and temperature patterns during the LIE season (Largier et al. 1997). For example, in a hypothetical LIE (Fig. 1B), the outer bay is characterized by newly upwelled waters and strong tidal mixing (high nutrients and cold water) that likely preclude phytoplankton biomass from accumulating, while the innermost bay is characterized by well-aged waters and weak tidal mixing (low nutrients and warm water) that also prevent phytoplankton from accumulating (but *see* Boyle et al. 2004). The middle bay, however, is characterized by intermediately aged waters and mixing rates (intermediate nutrients and warm water) that may allow phytoplankton to accumulate by retaining water long enough for primary production to exceed mixing but briefly enough that nearshore waters can replace nutrient-depleted waters. But, as the hypothetical estuary receives more freshwater input and as coastal upwelling subsides (Fig. 1A), the aforementioned oceanographic processes may weaken and thereby inhibit phytoplankton blooms in the bay during the non-LIE season.

Here we investigate how intense coastal upwelling combined with the tidal flux of a semi-enclosed bay (Tomales Bay) affect the growth of an estuarine benthic invertebrate, the Olympia oyster (*Ostrea lurida* = *Ostreola conchaphila*). Situated in an intense upwelling region, Tomales Bay, California (38°231′N, 122°978′W), is a 20 km–long and 1 km–wide linear basin that was tectonically formed by the San Andreas Fault (Hearn and Largier 1997). This LIE receives little freshwater inflow for much of the upwelling season and has a negative hydrological balance as a result of evaporation that exceeds freshwater inflow (Hearn and Largier 1997). The bay's hydrological balance is then expected to produce opposing gradients of retention time and nutrient availability that we predict will influence invertebrate growth by generating spatial gradients in temperature and phytoplankton (Hearn and Largier 1997; Largier et al. 1997). If consistent, these spatial gradients can also be used to test whether oyster growth in Tomales Bay is limited by temperature or phytoplankton (Menge et al. 2008).

The Olympia oyster is native to northeast Pacific estuaries. Like certain other benthic invertebrates, oysters are important prey and can also act as foundation species by providing a habitat that benefits the fitness and diversity

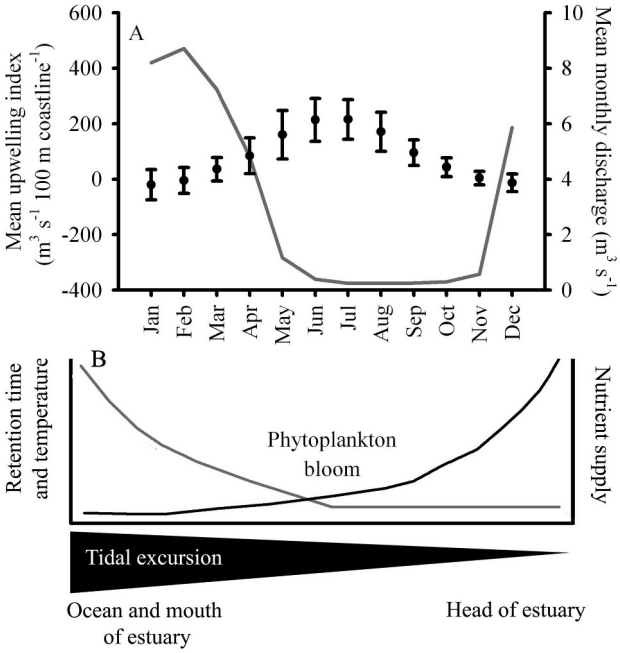

Fig. 1. (A) Black data points represent average monthly values (from 1967 to 1991) of historical upwelling index for 39°N–125°W (left y-axis). Gray line represents monthly averages of local freshwater discharge into Tomales Bay, California, from 2004 to 2008 (right y-axis). Data provided by National Oceanic and Atmospheric Administration–Environmental Research Division and the U.S. Geological Survey. (B) Map of hypothetical low-inflow estuary, illustrating how tidal excursion may lead to physical gradients in retention time and temperature (black line, left y-axis) as well as nutrient supply (gray line, right y-axis) that promote phytoplankton blooms during the summer upwelling season.

of other organisms (Bruno and Bertness 2001; Stachowicz 2001). In Tomales Bay, a remnant population of Olympia oysters still functions as a foundation species, despite being overharvested in the early 20th century (Kirby 2004; Kimbro and Grosholz 2006). But the oyster's importance as a habitat likely varies spatially, because oysters appear to be larger in the middle of the bay than elsewhere in the bay (D. L. Kimbro unpubl.). Although the link between coastal upwelling and the growth of foundation species along the outer coast has been examined (Menge and Branch 2001; Blanchette et al. 2007; Menge et al. 2008), considerably less research has investigated how the bottom-up effect of oceanography influences foundation species in estuaries.

The goal of our study was to understand how intensive coastal upwelling and tidal excursion affect oyster growth in Tomales Bay. Based on our unpublished observations of oysters in Tomales Bay, we suspected that high rates of oyster growth are supported in some locations of the bay and that these locations are determined by the interaction of freshwater inflow, upwelling, and tidal excursion. The specific objectives of our study were (1) to measure the tidal excursion during a LIE season and determine how the tidal excursion affects seasonal patterns of water residence times, nutrients, temperature, and phytoplankton; (2) to quantify

oyster size distributions and growth rates throughout the bay; (3) to examine whether spatial variation in oyster size and growth may be caused by the effects of tidal excursion and coastal upwelling on phytoplankton and water temperature; and (4) to determine whether oyster growth in Tomales Bay is limited by water temperature or phytoplankton.

Methods

Natural history of the Olympia oyster—The Olympia oyster is a protandrous hermaphrodite that is native to eastern Pacific estuaries from Alaska to Baja California Sur, Mexico (Baker 1995). After embryos are brooded within adult oysters for 10–14 d, planktotrophic larvae develop for 4–6 weeks during summer months before settling on hard substrate such as rocks and cobbles. Oysters can grow to ~6 cm in length and often create loose reefs (~0.10 m tall) in low intertidal and shallow subtidal portions of estuaries (Baker 1995). Because hard substrate is limited in soft sediment estuaries, oysters compete among themselves and with other sessile organisms for space on rocks. At the same time, the biogenic structure of Olympia oysters provides habitat for associated species, including amphipods and polychaetes as well as sponges and algae that attach to and live on the oysters (Kimbro and Grosholz 2006). Olympia oysters occur across broad areas of shoreline (~20 km) in Tomales Bay, with densities of up to 40 oysters 0.06 m^{-2}.

Estimating tidal excursion—To determine whether the tidal excursion decreases with distance from the mouth, as expected from one-dimensional mass–balance estimates (Largier et al. 1997; Harcourt-Baldwin and Diedericks 2006), we deployed three satellite-tracked surface drifters at each of three distances from the mouth encompassing most of the oyster's distribution (distances of 8, 12, and 16 km from the mouth; Fig. 2). Drifters free-floated between 0.5 and 1.5 m in water depth and were tracked via internal recording Garmin GPS units that recorded a position every 2 min; their design is described in detail (Davis 1985; Largier 2003). Given that Tomales Bay is well mixed and has negligible vertical shear currents (Largier et al. 1997; Harcourt-Baldwin and Diedericks 2006), these drifter trajectories adequately measure currents throughout the water column. For each distance from the mouth, three drifters were equidistantly deployed across the bay (¼, ½, and ¾ of the width), and a fourth drifter that lacked a GPS unit was also deployed at half width. All drifters were deployed on 02 August 2007 in less than 1 h during high tide. This day was chosen because of the symmetrical tidal cycle that started with a high tide of 1.77 m in the morning and ended with a high tide of 1.74 m in the afternoon. The symmetrical tide allowed two observations of excursion (one on flood and one on ebb) and also an assessment of tidal residual transport. Drifters at the 8-km site were deployed around 03:23 h, about 47 min after predicted local high tide water (HW); drifters at 12 km were deployed around 03:51 h, about 69 min after predicted local HW; and drifters at 16 km were deployed around 04:10 h, about 86 min after predicted local HW. Drifter trajectories were plotted and excursion was calculated as the maximum longitudinal displacement. The small-scale variability in the trajectories also demonstrates small-scale mixing (we only do so qualitatively here).

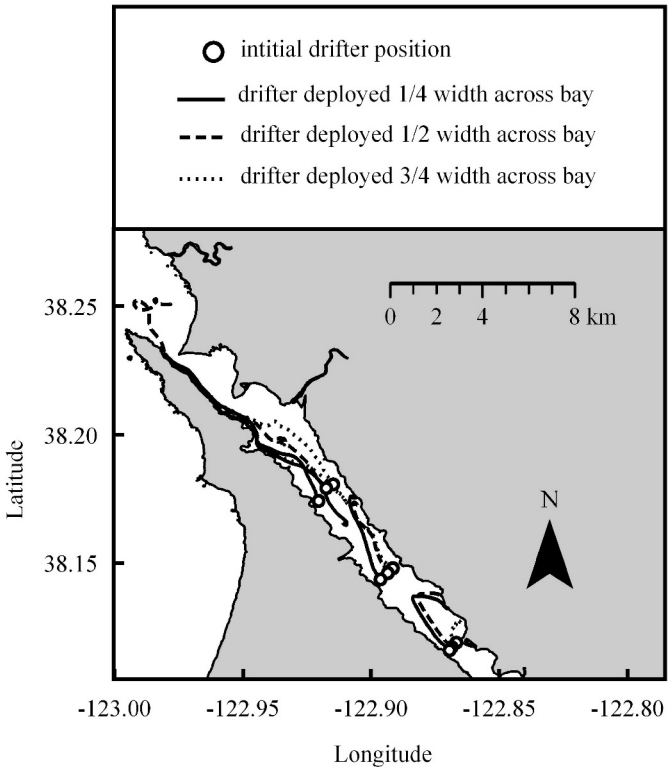

Fig. 2. Map of tidal trajectories for drifters in Tomales Bay that illustrates tidal excursions for three cross-sections within Tomales Bay: 8 km, 12 km, and 16 km from the mouth.

Seasonally varying physical and biological gradients—To determine whether spatial variation in tidal excursion produces longitudinal gradients in residence time, nutrients, phytoplankton, and temperature, we conducted monthly boat surveys from 2004 to 2008, during which conductivity–temperature–depth (CTD) profiles were obtained at 10 stations along the estuary (Fig. 3A). Using a SBE19plus CTD (Seabird-Electronic) fitted with a WET-Labs fluorometer, we sampled sites that were part of the Biogeochemical Reactions in Estuaries (BRIE) study conducted during the late 1980s and early 1990s (Smith et al. 1989; Largier et al. 1997). These sites were spaced 2 km apart, and profiles were sampled at 2 Hz (approximately four values per meter). Each monthly survey started at the mouth just before slack high tide and finished at Sta. 18 km about 15–30 min after local high tide (total time, ~1.5 h). We used the Bakun upwelling index (evaluated monthly for latitude 39°N since 1967; http://www.pfeg.noaa.gov/products/PFEL/modeled/indices/upwelling/NA/click_map.html) and U.S. Geological Survey data related to local freshwater discharge (monthly averages at head of Tomales Bay from 2004 to 2008; http://waterdata.usgs.gov/ca/nwis/dv/?site_no=11460600) to define the seasonality of upwelling and freshwater discharge for this region (*see* Fig. 1A). Consistent with these seasonal cycles, and as suggested by

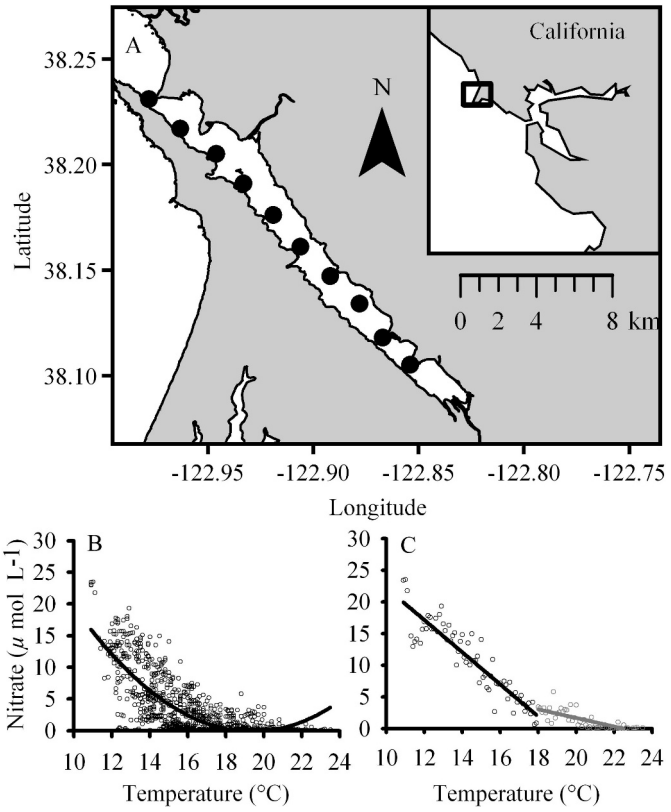

Fig. 3. (A) Map of 10 sampling stations (black dots) located every 2 km from the mouth to the head of Tomales Bay, California. (B) Quadratic fit of Nitrate vs. Temperature during low-inflow estuarine months from 1987 to 1995 in Tomales Bay, California. (C) Bilinear fit of maximum observed nitrate concentration vs. each observed temperature. Data obtained from http://lmer.marsci.uga.edu/tomales/ (Smith and Hollibaugh, LMER Coordinating Committee 1992). In panel C, black and gray symbols differentiate the data for each linear fit.

Largier et al. (1996), we grouped monthly salinity, temperature, and chlorophyll fluorescence data into two seasons, the LIE season (July–October) and the non-LIE season (November–June). Our seasonal categorization, however, is imperfect, as LIE conditions sometimes occur during May, June, and November. For each station, all data were then averaged to create seasonal salinity, temperature, and chlorophyll *a* (Chl *a*) means (±SD). In addition to monthly chlorophyll fluorescence data, we also sampled each station on four different days from 30 July 2007 through 06 August 2007 and throughout an entire low–high tidal cycle on 01 August 2007 to explore how tidal cycles may alter the spatial structure of a phytoplankton gradient by varying tidal excursion. To increase the spatial resolution of these data, we measured Chl *a* (via fluorescence) every 1 km between Sta. 6 km and Sta. 16 km.

Although water residence time and nutrient concentrations were not directly sampled, the salinity and temperature data provide a proxy for each parameter. Here, residence time indicates how long a composite parcel of water has been exposed to evaporative loss of freshwater (as well as being exposed to the light that fuels primary production). In this sense, it is perhaps better thought of as the "age" of the water since it was upwelled. Residence times (T_{res}) for each station were estimated with a bulk (Lagrangian) salt balance, thus:

$$T_{res} = (S - S_O)H_{av}/E_{av}S_{av} \quad (1)$$

where S_O represents ocean salinity, S represents the salinity of the specific site, H_{av} represents average water depth along the Lagrangian trajectory, E_{av} represents the evaporation rate, and S_{av} represents average salinity along the Lagrangian trajectory (Largier et al. 1997). S and average water depth (H_{av} = 8.11 m) were directly observed, and a value of 0.001 m d^{-1} was used for E (Largier et al. 1997). Because this salt balance assumes steady-state conditions, we estimated residence times only for the LIE season, when conditions change slowly and steady conditions are approximated (Largier et al. 1997). Although Tomales Bay typically displays LIE conditions between July and October, steady-state conditions sometimes occur during May, June, and November.

Nitrate is generally the limiting nutrient in upwelling systems (Dugdale et al. 2006) and specifically in this Tomales–Bodega region (Wilkerson et al. 2006). Historical data on nitrate concentrations and temperature are available from 1987 to 1995 for all stations in Tomales Bay (Smith et al. 1989). Assuming that nitrate and temperature are well correlated in recently upwelled waters (Dever et al. 2006), and because of similar rates of warming and greening of newly upwelled waters, we used these BRIE data to develop a temperature–nitrate relationship. This relationship is described by a quadratic function in the LIE season (Fig. 3B). We also obtained a bilinear curve that defines the maximum nitrate concentration observed during BRIE for a given water temperature: for temperatures over 18°C, nitrate will likely be ≤ 3 μmol L^{-1} (Fig. 3C) and near zero when temperatures exceed 22°C during the upwelling dry season. Based on this bilinear fit, we estimated nitrate concentrations from our monthly observations of temperature during the ocean-dominated LIE season in Tomales Bay.

Oyster size distributions—During the spring of 2006, we surveyed oyster sizes at multiple sites spanning the entire distribution of oysters in Tomales Bay (6–17 km distance from the mouth of the bay). After selecting equal-sized beaches (~300 m long) with suitable oyster habitat (intertidal rocks within +0.5 to −1.5 mean lower low water), we vertically divided each beach (relative to horizontal waterline) into three 100 m–long sections. Each section's oyster habitat was then horizontally bisected to create a high and low intertidal oyster zone paralleling the waterline (six zones per site). Within the middle of each high and low oyster zone, a 15-m horizontal transect was established and then centered in its respective 100-m section.

After partitioning each site's oyster habitat, we selected rocks along transects to sample for oyster densities. To avoid selecting rocks clustered at the end of transects, each 15-m transect was divided into two 7.5-m subtransects. We then marked all rocks occurring within 35 cm of the subtransects. The marked rocks in each subtransect were

tallied, and three rocks were randomly selected for survey, yielding six rocks per transect. For each rock, we centered a quadrat (10 × 10 cm) on the top, bottom, and side surfaces and measured the size of all oysters within each quadrat. Using a nonparametric test (Kruskal–Wallis rank scores), we then compared oyster size distributions among sites. We also used ordinary least squares (OLS) regression to examine the functional relationship between distance from ocean and oyster size. By comparing values of R^2 and employing a Partial F-statistic (Quinn and Keough 2002) we also determined whether a linear or quadratic line best fits this functional relationship.

Oyster growth experiment—To determine whether coastal upwelling and tidal excursion affect oyster growth by spatially varying phytoplankton and temperature, we conducted two different experiments at sites on the western shoreline of Tomales Bay. By spawning adult oysters at the Bodega Marine Laboratory, we settled juvenile oysters onto polyvinyl chloride tiles (10 × 10 cm). For the first experiment, we randomly assigned 36 tiles among three sites (sites W2 [8 km], W3 [12 km], and W4 [16 km]; tile $n = 9$) in July 2006. These sites encompass most of the oyster's distribution; the time of deployment coincides with the season of oyster recruitment; and the tile size is similar to the small cobbles commonly found at these sites (D. L. Kimbro unpubl.). Before deploying tiles, we marked five oysters per tile with small numbered tags (Floy Tags, FTF-69 Fingerling Tag-Pennant) and took digital photos of each tile. We then photographed all tiles monthly thereafter, although before taking photographs, we removed other sessile invertebrates and algae. Using image analysis software (Metamorph 6.0, Universal Imaging Corporation) we estimated individual size and growth rate for tagged oysters only. In this study, growth rate refers to the change in a tagged oyster's size between months from July to October 2006.

To better estimate important biotic and abiotic variables at each site at which oyster growth was measured, we deployed time-series sensors for chlorophyll fluorescence (WETLabs FLNTUSB-525 sampling every 5 min) and water temperature (SeaBird SBE39 sampling every 2 min) about 10 m offshore of the experimental sites. Although most data were of high quality, there was a recurrent spiking problem: repeated data with instrument maximum range values of 50 mg m^{-3}, which are too high and also form a distinct second peak in data distributions. Because the problem disappeared after installing new anti-fouling wiper blades, the original faulty blades likely caused the data problem. But without confidence that we could objectively remove all spikes, we calculated 48-h median values of Chl *a* for each site, which excluded any influence of these spikes. The 48-h medians were then used to obtain a monthly mean of Chl *a* as an estimate of food availability. While tidal fluctuations are not represented in 48-h median data, these records do provide a clear signal of variability on time scales sufficiently shorter than the key bloom and upwelling time scales that characterize the varying environments of food and temperature. Finally, we encountered further data problems when the fluorometer at site 16 km disappeared and the remaining fluorometers ceased recording data during the final month of the 2006 experiment. Thus, for September–October, we lack Chl *a* and temperature data for site 16 km.

Using a repeated-measures univariate ANOVA with modified degrees of freedom to account for the assumption of sphericity (Quinn and Keough 2002), we first tested whether differences in mean size and growth of oysters among sites (W2 [8 km], W3 [12 km], and W4 [16 km]) depended on time (i.e., sampling month). When significant Site × Time interactions were detected, we then used analysis of covariance (ANCOVA) and Tukey's post hoc comparison of means to test how site means differed within each month. In this analysis, the density of oysters (tagged + untagged) at each site was used as a covariate, because higher densities may increase competition for food or space among oysters that in turn may limit the growth of tagged oysters. Although our random assignment of tiles among sites initially produced higher densities at the 12-km site and prevented the covariate slopes among all three sites from initially being homogeneous, we proceeded with the ANCOVA because the covariate is an important biological effect of interest (Quinn and Keough 2002). For the remaining 2 months of the experiment, the covariate slopes were homogeneous. Among sites, this procedure produced three mean comparisons for oyster growth rates and four comparisons for oyster sizes. Variances involved in all comparisons were homogeneous. To investigate whether oyster growth rate depended on Chl *a* and temperature, we used a multiple linear regression (MLR) of monthly oyster growth rate as the dependent variable vs. monthly means of Chl *a* and temperature as independent variables. Because we lacked Chl *a* and temperature data for September–October, we excluded the September–October growth rate data from this MLR.

This 2006 experiment was repeated from July to August 2007; an outer bay site (6 km) on the western shoreline was added. Because this site generally has lower Chl *a* values than do middle bay sites, we felt that this additional experiment would increase the temporal and spatial scope of our results. For this second experiment, we used monthly CTD profile data to estimate mean Chl *a* and temperature values rather than the fluorometer and thermistor time series data, as in 2006. All other methods and statistical analyses remained the same as those in the 2006 experiment.

Although the moored fluorometer of the 2006 experiment provided higher resolution of how Chl *a* may vary among sites, it differed from the instrument used in the 2007 experiment and was also used in a different environment (shallow turbid nearshore waters). To avoid making invalid comparisons between numbers from the two different fluorescent sampling procedures, we do not use a standard conversion for the moored fluorometer data. Instead, we report these data in digital counts, which restricts comparisons among sites to within each year.

Results

Empirically estimating tidal excursion—In the 13-h study of tidal excursion, the distance that surface drifters traveled decreased with distance from the mouth (Fig. 2). During a moderate spring tide and calm winds, all drifters at the 8-

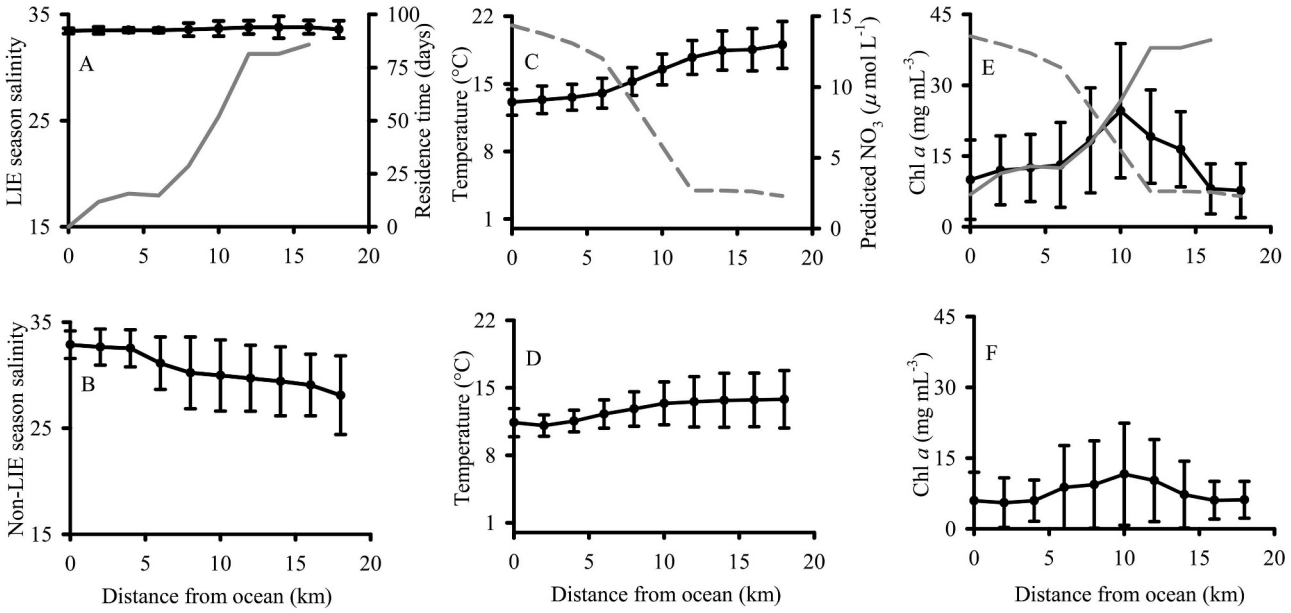

Fig. 4. Seasonal estimates from 2004 to 2008 of (A, B) salinity structure (black data points, mean ± SD, left y-axis) and estimated residence times (gray line, right y-axis); (C, D) temperature (black data points, mean ± SD, left y-axis) and estimated nitrate concentration (gray dashed line, right y-axis); and (E, F) phytoplankton biomass (Chl *a*, black data points, mean ± SD) across sites. Panel E includes predicted residence times (gray solid line) and nitrate concentrations (gray dashed line) to illustrate how they may interact to influence Chl *a* concentration in the middle of the bay.

km site were transported beyond the mouth of the estuary during the ebb tide; two drifters turned about 1 km beyond the mouth and returned to the bay, one drifter was recovered outside of the bay, and the fourth drifter was lost outside the bay. In contrast to this large tidal excursion, drifters released at the 12-km site moved a little over 3 km on the ebb tide. But this appears to be an underestimate, because the 12-km drifters snagged on seagrass in shallow waters along the east shore. This seagrass effect was directly observed and can also be deduced from the drifters' slowing pace before slack water (i.e., the distance between successive positions decreased). The drifters' collective trajectory toward the east shore is also consistent with a westerly sea breeze that crested the ridge west of the bay only where the ridge was low, which was at the middle bay (personal observations logged during fieldwork). Because wind has little direct influence on drifters, this westerly sea breeze indirectly affected the drifter's trajectory by modifying water circulation and pushing the near–surface water toward the eastern shore. As a result, the westerly winds did not affect drifters released at 8 km and only weakly influenced drifters released at 16 km. Finally, the drifters released at the 16-km site were transported only 2.5 km and did not reach the seagrass bed on the eastern shore until well after the low-water slack tide.

On the subsequent flood tide, 8-km drifters moved back into the bay with an excursion of 9–10 km. The 12-km drifters remained in the seagrass, while the 16-km drifters moved landward 1–2 km before also becoming entangled in seagrass along the east shore. For all locations landward of 6 km, the drifters' smooth trajectories indicate that the lack of complex topography allowed drifters to experience minimal small-scale eddy mixing during tidal advection (Hearn and Largier 1997; Largier et al. 1997). In contrast, drifters that moved beyond the mouth exhibited significant eddy behavior, indicating strong mixing of Tomales Bay waters with ambient Bodega Bay waters.

Seasonally varying physical and biological gradients—From 2004 through 2008, salinity and temperature for the entire estuary varied seasonally, as expected (Largier et al. 1997). In non-LIE seasons, means (±SD) of salinity and temperature were relatively low (30.9°C ± 2.9°C and 12.3°C ± 2.2°C, respectively) compared to LIE seasons (33.6°C ± 0.5°C and 15.4°C ± 2.6°C, respectively). In addition, salinity and temperature varied spatially as a function of distance from the ocean. In the absence of significant freshwater input during LIE seasons, salinity remained constant or increased slightly with distance from the mouth of the estuary (Fig. 3A). But with significant freshwater inputs at the head of the estuary during non-LIE seasons, salinity decreased with distance from the mouth of the estuary (Fig. 4B). For both seasons, temperature increased with distance from the mouth of the bay (Fig. 4C,D) because of the import and heating of upwelled water in the bay.

Averaged over the entire estuary, Chl *a* concentrations were higher during LIE seasons (15.4 ± 11.0 mg m^{-3}) than in non-LIE seasons (7.4 ± 7.5 mg m^{-3}; Fig. 4E,F). During LIE seasons, Chl *a* concentrations were highest in the middle bay (24.6 ± 14.2 mg m^{-3}). This middle bay maximum was also seen in a few non-LIE months, when there was an early decrease in runoff and an increase in upwelling (e.g., March 2006) or when there was a delay in the onset of freshwater input (e.g., November 2004). This

interannual variability in the months exhibiting LIE conditions means that some mid-bay LIE phytoplankton maxima are observed in the nominal non-LIE months of November through June that in turn artificially increased the non-LIE average of Chl *a* maximum.

The LIE season Chl *a* spatial pattern was consistent with the longitudinal patterns in residence time (Fig. 4A) and nitrate concentration (Fig. 4C). While the outer bay was characterized by newly upwelled high-nitrate waters and short residence times, the inner bay was characterized by low nitrate levels and long residence times; high Chl *a* levels were found in the middle bay, where waters had moderate levels of nitrate and moderate residence times. Throughout a portion of the spring-neap tidal cycle in the 2007 summer (30 July–06 August), the Chl *a* maximum persisted in the middle of the bay between 12 and 14 km and increased in magnitude (Fig. 5A). Meanwhile, during the high–low tidal cycle phase on 01 August 2007, the Chl *a* maximum at low tide spanned from 8 to 14 km (Fig. 5B). Because of advective import of coastal (Bodega Bay) waters, this Chl *a* maximum was reduced and then truncated between 12 and 14 km by the incoming and high tides, respectively (Fig. 5B).

Oyster size distributions—According to the nonparametric Kruskal–Wallis Test (Chi-square = 598.49, $p < 0.0001$), oyster distributions at middle bay sites are skewed toward larger sizes (positive values of [Mean − Mean0]/Std0) relative to those at inner bay sites (negative values of [Mean − Mean0]/Std0; Fig. 6A). For example, sites W1 and E1 have means (±SD) of 49.7 ± 7.9 mm and 53.7 ± 9.7 mm, respectively. In contrast, sites W5 and E4, which are farther from the mouth of the bay, have distributions skewed toward smaller oyster sizes (33.0 ± 7.1 mm and 30.9 ± 7.2 mm, respectively). In an OLS regression, oyster size was negatively correlated with distance from the mouth of the bay ($y = -1.97x + 65.49$, $R^2 = 0.33$, $p < 0.0001$). But according to the Partial *F*-test ($F_{1,1479} = 308.57$, $p < 0.0001$), this negative relationship is asymptotic (Fig. 6B).

Oyster growth experiment—During the first experiment (2006), site differences in the size of tagged oysters varied with time (repeated-measures ANOVA, univariate G-G Epsilon $F_{3.85,44.33} = 30.48$, $p < 0.001$; Fig. 6A). Although sizes of tagged oysters were similar across sites at the beginning of the experiment ($F_{2,24} = 0.35$, $p = 0.71$), 1 month later, oysters were 50% larger at the 12-km site than at the 8-km and 16-km sites ($F_{2,24} = 18.81$, $p < 0.001$; Tukey's post hoc test = 2.50; Fig. 7A). This size difference between the 8-km and 12-km sites, however, diminished over time. After 4 months of growth, oysters at the 8-km and 12-km sites were equal in size but larger than oysters at the 16-km site (October $F_{2,23} = 47.46$, $p = 0.001$, Tukey's post hoc test = 2.50; Fig. 7A).

Underlying these oyster size results, the growth rate of tagged oysters among sites also varied with time (repeated-measures ANOVA, univariate G-G Epsilon $F_{3.96,43.59} = 5.15$, $p < 0.002$). In the first month of the experiment, oyster growth rate at the 12-km site (W3, 0.77 ± 0.05 cm, least-squares mean ± SE) doubled that of oysters at the 8-km (W2) and 16-km sites (W5) (ANCOVA, $F_{5,21} = 23.49$, $p < 0.001$; Site $F_{2,21} = 51.41$, $p < 0.0001$; Tukey's post hoc test = 2.50, $p < 0.05$; Fig. 7B). Interestingly, the covariate of increasing oyster density was associated with decreasing growth rate at the 8-km and 16-km sites, but not at the 12-km site (Density covariate $F_{1,21} = 11.58$, $p < 0.005$; Site × Density $F_{2,21} = 8.14$, $p < 0.005$). Throughout the rest of the experiment, monthly growth increments at the 8-km site increased linearly, while those of the 12-km and 16-km sites did not change. As a result, oyster growth at the 8-km and 12-km sites were equal to each other and higher than that of the 16-km site during the second month ($F_{2,23} = 18.67$, $p = 0.001$, Tukey's post hoc test = 2.51) and third month ($F_{2,22} = 11.98$, $p = 0.003$, Tukey's post hoc test = 2.50).

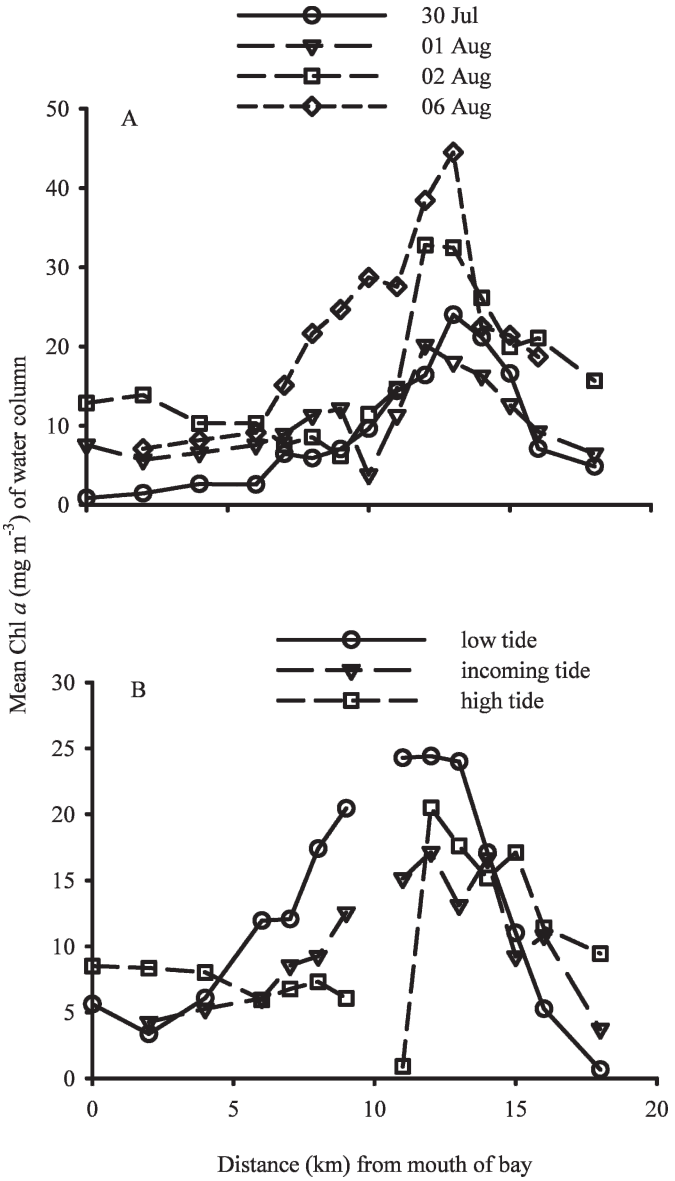

Fig. 5. (A) Daily variation in magnitude and position of Chl *a* peak throughout Tomales Bay over a week (30 July–06 August 2007). High tides increased each day: 30 July (1.33 m), 01 August (1.47 m), 02 August (1.55 m), and 06 August (1.76 m). (B) Variation in magnitude and position of Chl *a* peak throughout Tomales Bay during high–low tidal cycle phase of 01 August 2007.

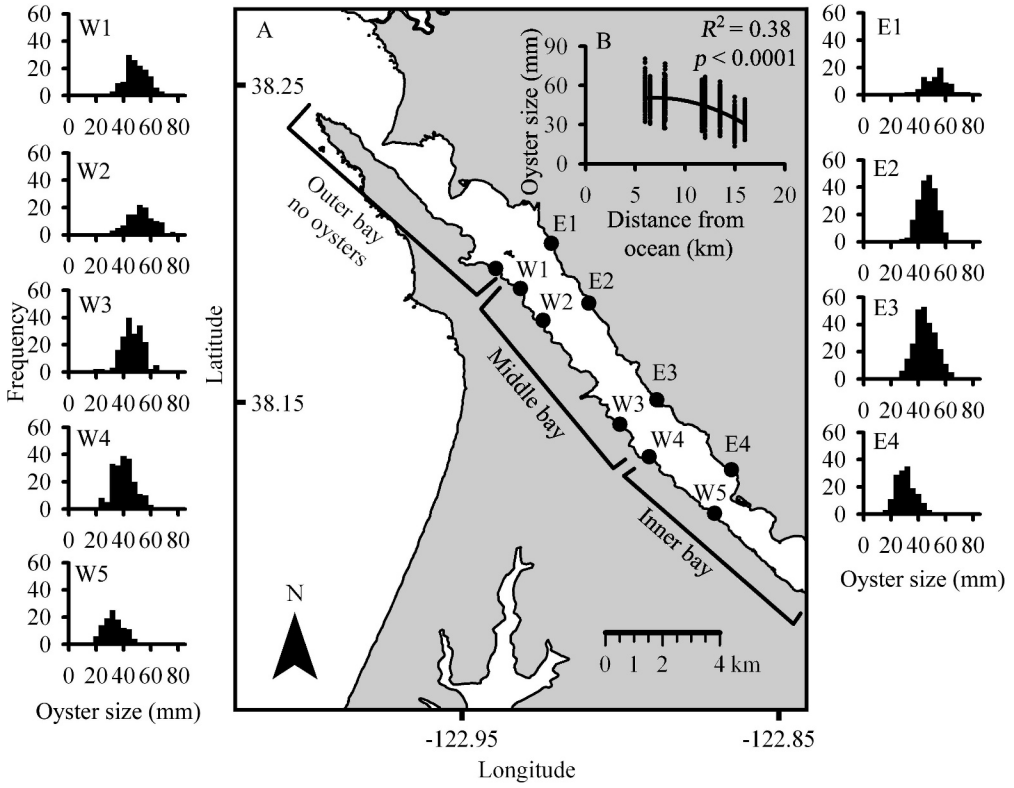

Fig. 6. (A) Size distributions of oysters throughout Tomales Bay, California, in 2006. (B) Plot of oyster sizes at each site vs. distance (km) of the site from the mouth of the bay ($y = -0.26x^2 - 1.79x + 66.95$).

For the last 2 months of the experiment, the covariate of oyster density was insignificant ($F_{1,19} = 2.55$, $p = 0.13$; $F_{1,18} = 3.75$, $p = 0.07$, respectively), and slopes of the covariate among sites were homogeneous ($F_{2,19} = 0.76$, $p = 0.48$; $F_{2,18} = 2.93$, $p = 0.08$, respectively).

While oyster growth rates can be influenced by both Chl *a* and temperature, the spatial distributions of Chl *a* and temperature contrasted sharply. Fluorescence data indicated that Chl *a* concentrations were highest at the 12-km site in July–August, highest at the 8-km site in August–September, and were consistently the lowest at the 16-km site (Fig. 7C). In contrast, water temperature was consistently highest at the 16-km site throughout the experiment (Fig. 7D).

When we added an additional site (6 km) and repeated the experiment from July to August 2007, differences in the size of oysters among sites again varied with time (repeated-measures ANOVA, univariate G-G Epsilon $F_{3,16} = 16.08$, $p < 0.0001$; Fig. 7E). At the beginning of the experiment, oyster size was equal at all sites except for the 6-km site, which was unintentionally given slightly smaller oysters (ANOVA, $F_{3,16} = 3.61$, $p = 0.03$, Tukey's test = 2.86). One month later, oysters were significantly larger at the 12-km site than at all other sites ($F_{3,16} = 12.48$, $p = 0.0002$, Tukey's test = 2.86). During one month, oysters at the 12-km site also grew significantly more than oysters at all other sites ($F_{3,16} = 15.82$, $p < 0.0001$, Tukey's test = 2.86; Fig. 7F); the covariate of oyster density was not significant (Density $F_{1,16} = 1.75$, $p = 0.21$). In addition to these size and growth rate differences, the ordering of the Chl *a* and temperature means also paralleled those of the July–August 2006 data (Fig. 7G,H). Finally, the 6-km site had the lowest Chl *a* concentrations and temperatures (Fig. 7G,H).

A MLR that used Chl *a* and temperature as independent variables accounted for 92% of the variance in oyster growth in 2006 (R^2 adjusted = 0.87, $F_{2,3} = 17.67$, $p = 0.02$). Although increasing leverages of Chl *a* concentrations significantly explained increasing leverage residuals of oyster growth rates ($F_{1,3} = 30.53$, $p = 0.01$; Fig. 8A), increasing leverages of temperature explained little variation in leverage residuals of oyster growth ($F_{1,3} = 1.8$, $p = 0.27$; Fig. 8B). For July–August 2007, the dependence of oyster growth on Chl *a* and temperature in a MLR was similar to that of 2006 ($R^2 = 0.99$, R^2 adjusted = 0.99, $F_{2,1} = 521.44$, $p = 0.03$; Chl *a* $F_{1,1} = 849.28$, $p = 0.02$; Temperature $F_{1,1} = 38.95$, $p = 0.10$; Fig. 8C,D). Temperature, however, was negatively associated with increasing oyster growth (Fig. 8D).

Discussion

Our data indicate that intense upwelling, freshwater discharge, and tidal mixing in LIEs can strongly influence benthic invertebrate populations. We found that during LIE conditions (July–October, Fig. 1A), a large tidal excursion frequently mixes the outer waters of Tomales Bay (Fig. 2) with nutrient-rich coastal waters, causing short residence time, high nutrient concentrations, and low temperatures (Fig. 4A–C). At the same time, a small tidal excursion infrequently mixes the inner portions of the

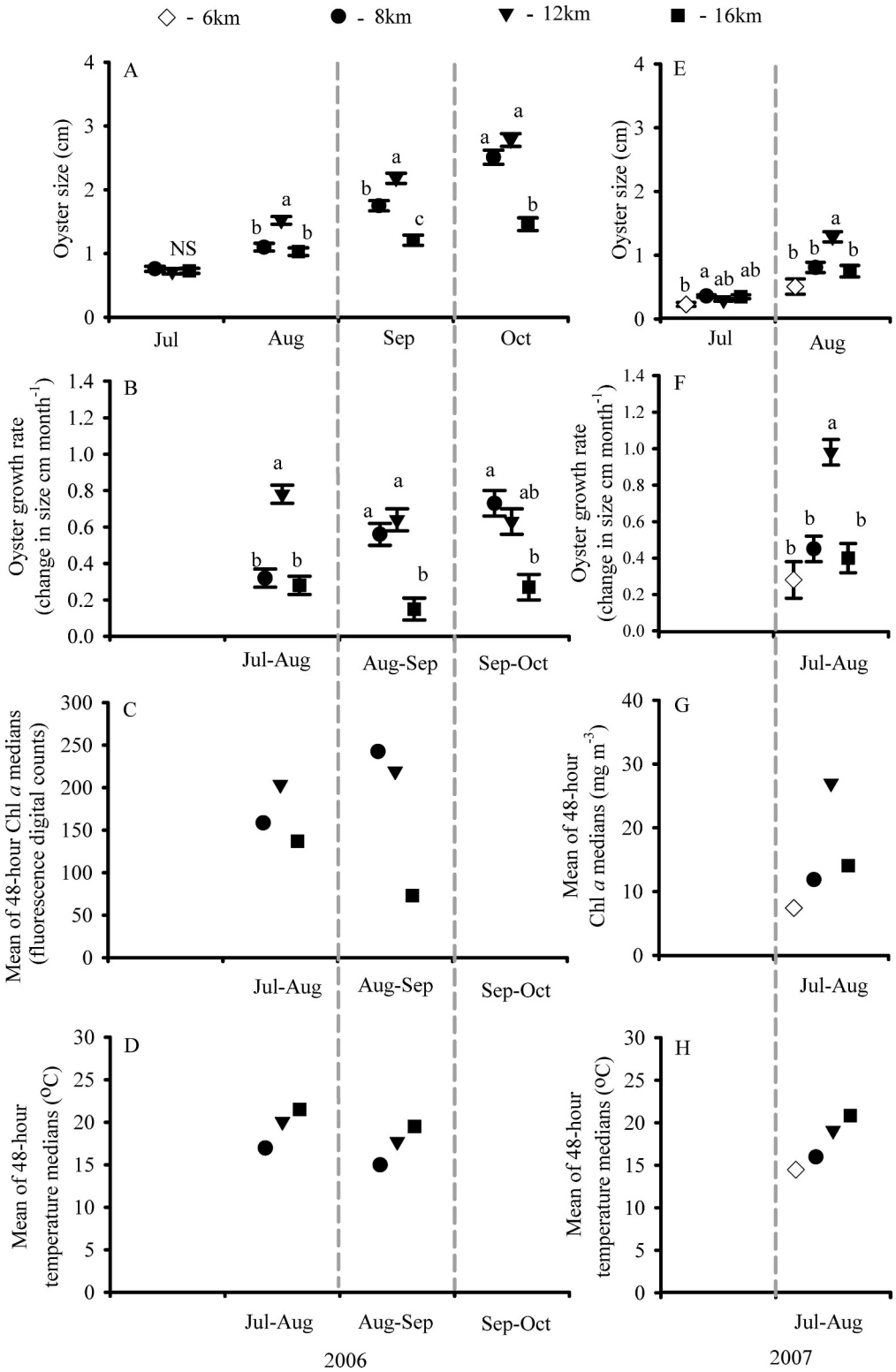

Fig. 7. Results of oyster growth experiments from (A–D) 2006 and (E–H) 2007. (A, E) Oyster size (mean ± SE) through time at sites within Tomales Bay: 6 km (only 2007 experiment, open circle), 8 km (closed circle), 12 km (triangle), and 16 km (square) from the mouth of the bay. (B, F) Oyster growth (mean ± SE) at each site through time. (C, G) Mean Chl *a* concentration at each site through time. (D, H) Mean temperature at each site through time. Significant differences among means indicated by differing letters (ANOVA and Tukey's post hoc test). In (B), least-square means (±SE) of oyster growth rate presented for July–August data because of a significant covariate effect.

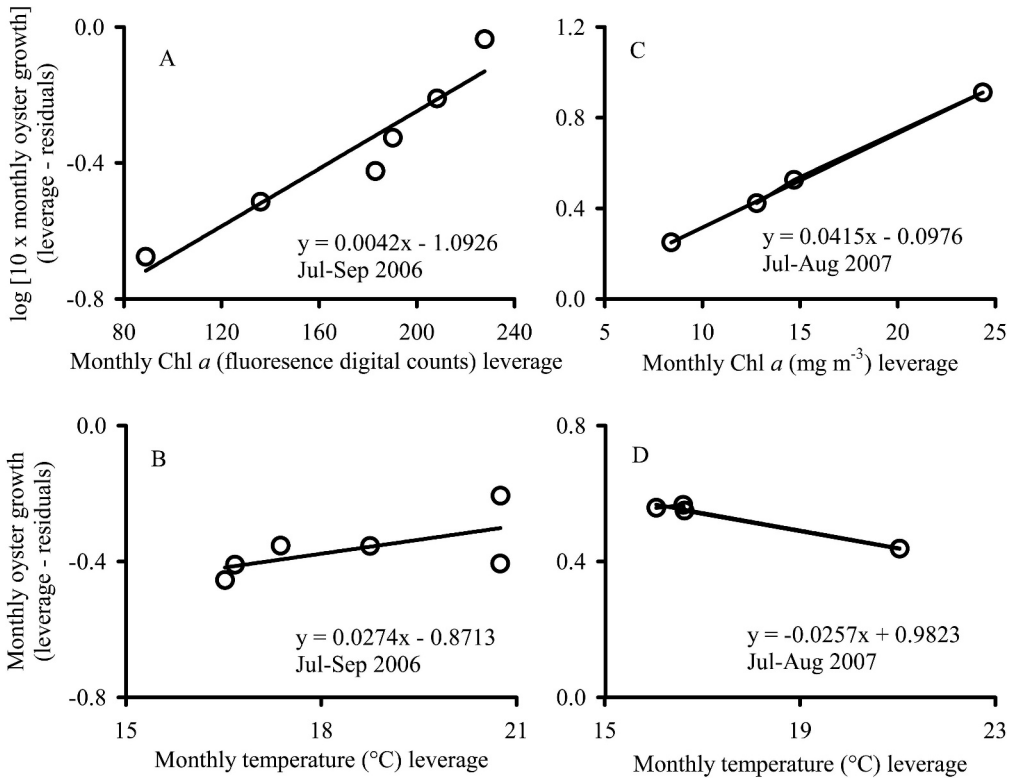

Fig. 8. Leverage plots of multiple linear regressions that used Chl *a* and temperature as independent variables to predict monthly growth of juvenile oysters at each site in (A, B) 2006 and (C, D) 2007.

estuary with coastal waters, causing long residence time, low nutrient concentrations, and higher temperatures (Fig. 4A–C). An intermediate tidal excursion, however, appears to sufficiently mix the middle bay and coastal waters, causing conditions (moderate residence time, moderate nutrient concentrations, and moderate temperatures) that support phytoplankton blooms (Fig. 4A,C,E).

Responding more to the unimodal–spatial structure of phytoplankton than to the linear–spatial structure of temperature during LIE conditions, juvenile oysters grew faster in the middle than in the outer and inner bays (Fig. 7B,F). But, as freshwater input increased and upwelling decreased during non-LIE months (Fig. 1A), phytoplankton blooms were not supported, and monthly growth of oysters across the entire estuary decreased by 30% (Fig. 4B,D,F; D. L. Kimbro unpubl.). Therefore, spatially varying growth rates due to LIE conditions are an important component in explaining why oysters are larger in the middle bay than in the inner bay (Fig. 6A,B). Growth rates alone, however, may not fully explain the population dynamics of oysters throughout the bay. For example, in the middle bay predation is higher at W2 (8 km) than at W3 (12 km, D. L. Kimbro unpubl.), which may help W2 oysters reach adult sizes that are slightly larger than those of W3 oysters by reducing oyster densities and competition for space. Because smaller oysters are more susceptible to predators, we also suspect that higher densities of marine predators coupled with low growth and low recruitment may explain why oysters are absent from the outer bay (Fig. 6A). Nevertheless, populations of smaller oysters provide less biogenic habitat for obligate organisms than do larger oysters (Kimbro and Grosholz 2006). Thus, a predictable supply of phytoplankton caused by an interaction between upwelling, freshwater discharge, and tidal excursion may allow middle bay oysters to support greater intertidal diversity and therefore to function better as a foundation species than inner bay oysters.

Three methodological and experimental limitations may affect the interpretation of our results. First, we did not comprehensively explore how variability in tides (high–low and spring-neap) and winds (local and offshore) affect the spatial distribution of phytoplankton and its link to oyster growth by altering the tidal excursion gradient. With respect to tides and tidal excursion, we only presented one set of tidal excursion observations from a moderately strong spring tide. But because tidal excursion is a deterministic process that varies linearly with the tidal range of Tomales Bay (Harcourt-Baldwin and Diedericks 2006), we can infer how the spring-neap tidal cycle affects the tidal excursion gradient. For example, the observed 4-km excursion at the 12-km site (Fig. 2) would increase to a 6-km excursion with a range of 2.29 m on a spring tide and decrease to a 2-km excursion with a range of 0.76 m on a neap tide. Furthermore, given that mixing rates vary with the square of tidal excursion (Largier et al. 1997), we also expect mixing rates to vary by a ninefold measure between neap and spring tides. Thus, a stronger spring tide and tidal excursion may simultaneously deliver nitrate and dilute phytoplankton concentrations farther into the bay, while

weaker neap tides may have the opposite effects. From this reasoning and observations of another low-inflow estuary (Chadwick and Largier 1999), we deduce that Tomales Bay contains maximum nitrate loads following spring tides and develops maximum phytoplankton loads during subsequent neap tides. Whether this deduction fully accounts for variation in the magnitude and spatial distribution of phytoplankton maximums (e.g., Fig. 5A) will be explored in a forthcoming modeling paper.

In addition to the spring-neap tidal cycle, our study did not fully address that a tidal excursion also comprises an influential high–low tidal cycle whose stage may determine where phytoplankton bloom in the bay (e.g., Fig. 5B). Given the limited eddy mixing of the middle bay as the tide recedes, our observed phytoplankton maximum could be advected toward the mouth of the bay and diluted by the strong mixing rates associated with the tidal pumping at the mouth (i.e., waters seaward of 8 km). In contrast, a strong incoming tide may dilute phytoplankton concentrations landward of 8 km. As a result, sampling at lower amplitude tidal cycles would likely show phytoplankton maximums remaining at the 12-km site and extending to the 8-km site, while sampling at higher tides would show a spatial contraction of phytoplankton maximums around the 12-km site. While this reasoning was supported by our results (Fig. 5B), we can only qualitatively address it in this study.

The less predictable variability of winds could also directly and indirectly influence our phytoplankton and tidal excursion results. We suspect that the most important influence of wind is on upwelling, which could indirectly affect the source and spatial distribution of phytoplankton as well as temperature in Tomales Bay. When northerly upwelling winds are strong, cold and high-nitrate waters are upwelled along the coast and are available for importation into Tomales Bay (Dever et al. 2006). In contrast, when upwelling relaxes for multiday periods, the coastal waters off Tomales Bay may be 'aged upwelled' waters or a combination of aged upwelled waters and San Francisco Bay–influenced waters (Largier et al. 2006), thereby providing a source of phytoplankton-rich and warm waters that can be tidally mixed into Tomales Bay (Banas et al. 2007). Such changes in ambient waters that persist for several days may significantly vary the longitudinal patterns of nutrients, phytoplankton, and temperature within Tomales Bay. While this scenario may sometimes be observed for Tomales Bay, a record of water temperatures at the 2-km site in 1992 indicates that sufficiently aged, upwelled waters are unusual at or near the mouth of Tomales Bay (J. Largier unpubl.).

In contrast to the indirect effect, a direct effect of wind was captured in the 1-d drifter experiment (Fig. 2). When the cool marine layer crested the west ridge of Tomales Bay, a westerly breeze blew across the bay. Based on the observed drifter tracks, this wind imparted a surface velocity toward the lee shore. While this complicates water-parcel trajectories, we suggest that the along-bay tidal motions still dominate the mixing and residence dynamics of water in Tomales Bay. For instance, north–south upwelling winds consistently blow landward along the longitudinal axis of the bay and pile up water at the southern end of the bay. Despite this stronger direct effect of north–south winds, bay waters still move landward and seaward with the tide. Thus, tidal excursion still operates in the presence of strong and direct wind effects. Although the regularity of these along-bay winds and irregularity of westerly winds may help maintain a mixed water column in Tomales Bay, we cannot assess that with our data.

A second limitation of our study is that we did not quantify whether grazing pressure from zooplankton or filter-feeding invertebrates varies spatially, which could have contributed to variation in phytoplankton abundance and therefore Olympia oyster growth. Previous research, however, has indicated that estuarine zooplankton abundances within the inner bay (i.e., 14–18 km) are low when middle bay phytoplankton peak (Kimmerer 1993). With respect to filter-feeding invertebrates, cultivated oysters (*Crassostrea gigas*) that consume phytoplankton occur at the head of the estuary (18 km) and at several sites in the middle bay (8 km and 13 km). In addition, Olympia oysters and other filter-feeding invertebrates such as mussels, barnacles, tunicates, and sponges occur throughout the middle and inner bays. Based on these invertebrate distributions, it appears that grazing pressure cannot fully explain why phytoplankton abundance is lower in the inner bay and higher in the middle bay. In contrast, outer bay waters contain cultivated oysters and high abundances of neritic zooplankton during upwelling (Kimmerer 1993). Thus, zooplankton and cultivated oysters may contribute to phytoplankton biomass being lower in the outer bay vs. the middle bay. Although we failed to quantify grazing pressure in the outer bay, Olympia oysters do not occur in the outer bay, and exceptionally high levels of Chl *a* still occur in the middle bay. Consequently, grazing pressure in the outer bay exerts little influence on how tidal excursion and coastal upwelling affect the growth of native Olympia oysters in the middle and inner bays.

A third limitation of the study is that we relied solely on phytoplankton quantity (Chl *a* mg m^{-3}) without considering phytoplankton quality (i.e., community composition). For example, we expect that diatoms are more common in the outer bay and that dinoflagellates are more common in the inner bay (Cole 1989). In the last month of our field experiment, we began a 12-month monitoring study that used high-performance liquid chromatography to characterize the community composition of phytoplankton species across our three experimental sites. From these preliminary data, we found consistent levels of diatoms at each site throughout the year. Spatial and temporal peaks in dinoflagellates, however, appear to coincide with higher oyster growth (M. Waters and D. L. Kimbro unpubl.). Therefore, phytoplankton composition (i.e., dinoflagellates or a diatom–dinoflagellate mixture) may also account for differences in oyster growth rates.

While our study has limitations, we still consistently found middle bay phytoplankton maximums and inner bay temperature maximums during LIE months, patterns that can be explained by the observed tidal excursion gradient. Further, our results indicate that by supporting seasonal peaks in phytoplankton, the intermediate tidal excursion of the middle bay also interacts with coastal upwelling to support larger, faster-growing oysters. Consequently, anoth-

er strength of our study is that it addressed whether upwelling and tidal excursion during LIE conditions increase oyster growth more through their effects on phytoplankton or temperature. Because invertebrate metabolic rates increase with temperature and because upwelling reduces water temperature, some researchers have argued that the growth and size of benthic invertebrates is limited more by temperature than by the upwelling of nitrates and the production of phytoplankton (Sanford and Menge 2001; Blanchette et al. 2007). Increasing water temperature in our study, however, failed to directly affect the growth of juvenile oysters for two consecutive years (Figs. 7, 8) and appears inversely related to the size structure of oyster populations (Fig. 6A,B). We suggest that physical features that retain upwelled waters, such as upwelling shadows and LIEs, may help reconcile our results with those of previous coastal studies. In the absence of physical mechanisms that retain water, we agree that the growth and size of benthic invertebrates would be negatively correlated to upwelling intensity. But we suggest that the positive relationship between upwelling intensity and growth that is mediated through upwelling's effect on phytoplankton is more causative in locations like Tomales Bay and upwelling shadows. In addition to illustrating how intense upwelling may increase benthic invertebrate growth, low-inflow bays like Tomales are useful for testing the relative importance of phytoplankton vs. temperature for invertebrate growth because phytoplankton and temperature are positively correlated from the outer bay to the middle bay and negatively correlated from the middle bay to the inner bay.

Within upwelling regions, our study is not the first to demonstrate a benthic–pelagic link between coastal upwelling and estuaries. In fact, Banas et al. (2007) recently used a circulation model to demonstrate that intermittent upwelling can lead to coastal phytoplankton being imported into and subsidizing a LIE in Washington—a result also observed in San Quentin Bay, Mexico (Camacho-Ibar et al. 2003). The ensuing spatial pattern of this oceanic phytoplankton may help explain why cultivated oyster (*C. gigas*) sizes decline with distance from the ocean (Banas et al. 2007). In contrast, by experimentally demonstrating how the spatial pattern of estuarine phytoplankton influences an oyster's ecological vital rate (i.e., growth), we mechanistically illustrate how upwelling and tidal excursion may cause Olympia oyster sizes to asymptotically decrease with distance from the mouth of the bay. This benthic–pelagic link also differs from that of Banas et al. (2007) because it is more characteristic of bays near persistent upwelling centers, where the bay is subsidized not by particulate organic matter but by dissolved inorganic nutrients that in turn fuel phytoplankton blooms within the bay. Thus, we suggest that benthic–pelagic links between coastal upwelling and LIEs may not be uniform throughout an eastern boundary current region with varying upwelling regimes. Further, these benthic–pelagic links will likely change as a function of anthropogenically and naturally induced variation in the upwelling wind climate as well as the loading of nutrients into west coast estuaries (Harley et al. 2006).

In conclusion, prior research has established that energy inputs from coastal upwelling can strongly influence the dynamics of rocky intertidal food webs (Menge and Branch 2001). More recent research has even shown that such inputs can also affect a LIE system (Banas et al. 2007). Complementing these results, our study directly links coastal upwelling to the population dynamics of an estuarine foundation species. In addition to highlighting an under-appreciated link between upwelling and the tidal excursion of a LIE, our results also indicate that although the growth of benthic invertebrates may often respond more to water temperature than to upwelling and phytoplankton (Blanchette et al. 2007; Menge et al. 2008), there are important exceptions.

Acknowledgments

We thank R. Hughes, B. Jaffee, J. Stachowicz, C. Finelli, and two anonymous reviewers for comments and ideas that improved this manuscript. S. Attoe, A. Baukus, N. Bosch, J. Byrnes, H. Carson, A. Chang, I. Clarke, C. Coleman-Hulbert, M. Ferner, J. Fisher, R. Kordas, N. Nesbitt, K. Nickols, S. Morgan, M. O'Leary, S. Peters, P. Reynolds, M. Sheridan, and B. Steves generously provided field assistance and equipment. We also thank B. Steves for helping produce the manuscript's figures. This research was supported by grants from the University of California (UC) Marine Council/Coastal Quality Environmental Initiative (to D.L.K.), UC Davis Graduate Group in Ecology (to D.L.K.), National Park Service at Point Reyes National Seashore (to D.L.K.), National Oceanic and Atmospheric Administration (to E.D.G.), National Parks Service–California Cooperative Ecosystem Studies Program (to E.D.G.), Pacific States Marine Fisheries Commission (to E.D.G.), UC Exotic/Invasive Pest and Disease Program (to E.D.G.), California Sea Grant Program (Grant R/ENV-203 to E.D.G.), and National Science Foundation–Research Experience for Undergraduates (Grant DBI0453251 to N.J.N. and N.M.T.). This paper is contribution number 2444, Bodega Marine Laboratory, University of California–Davis.

References

Baker, P. 1995. Review of ecology and fishery of the Olympia oyster, *Ostrea lurida* with annotated bibliography. J. Shellfish Res. **14:** 501–518.

Banas, N. S., B. M. Hickey, J. A. Newton, and J. L. Ruesink. 2007. Tidal exchange, bivalve grazing, and patterns of primary production in Willapa Bay, Washington, USA. Mar. Ecol. Prog. Ser. **341:** 123–139.

Blanchette, C. A., B. Helmuth, and S. D. Gaines. 2007. Spatial patterns of growth in the mussel, *Mytilus californianus*, across a major oceanographic and biogeographic boundary at Point Conception, California, USA. J. Exp. Mar. Biol. Ecol. **340:** 126–148.

Boyle, K. A., K. Kamer, and P. Fong. 2004. Spatial and temporal patterns in sediment and water column nutrients in a eutrophic southern California estuary. Estuaries **27:** 378–388.

Broitman, B. R., and B. P. Kinlan. 2006. Spatial scales of benthic and pelagic producer biomass in a coastal upwelling ecosystem. Mar. Ecol. Prog. Ser. **327:** 15–25.

Bruno, J. F., and M. D. Bertness. 2001. Habitat modification and facilitation in benthic marine communities, p. 201–218. *In* M. D. Bertness, S. D. Gaines and M. E. Hay [eds.], Marine community ecology. Sinauer Associates.

Camacho-Ibar, V. F., J. D. Carriquiry, and S. V. Smith. 2003. Non-conservative P and N fluxes and net ecosystem production in San Quintin Bay, Mexico. Estuaries **26:** 1220–1237.

Chadwick, D. B., and J. L. Largier. 1999. The influence of tidal range on the exchange between San Diego Bay and the ocean. J. Geophys. Res. Oceans **104:** 29885–29899.

Cole, B. E. 1989. Temporal and spatial patterns of phytoplankton production in Tomales Bay, CA, USA. Estuar. Coast. Shelf. Sci. **28:** 103–115.

———. 1989. Temporal and spatial patterns of phytoplankton production in Tomales Bay, CA, USA. Estuar. Coast. Shelf. Sci. **28:** 103–115.

Davis, R. E. 1985. Drifter observations of coastal surface currents during code—the method and descriptive view. J. Geophys. Res. Oceans **90:** 4741–4755.

Dever, E. P., C. E. Dorman, and J. L. Largier. 2006. Surface boundary-layer variability off Northern California, USA, during upwelling. Deep-Sea Res. II **53:** 2887–2905.

Dugdale, R. C., F. P. Wilkerson, V. E. Hogue, and A. Marchi. 2006. Nutrient controls on new production in the Bodega Bay, California, coastal upwelling plume. Deep-Sea Res. II **53:** 3049–3062.

Graham, W. M., and J. L. Largier. 1997. Upwelling shadows as nearshore retention sites: The example of northern Monterey Bay. Cont. Shelf Res. **17:** 509–532.

Harcourt-Baldwin, J. L., and G. P. J. Diedericks. 2006. Numerical modelling and analysis of temperature controlled density currents in Tomales Bay, California. Estuar. Coast. Shelf Sci. **66:** 417–428.

Harley, C. D. G., and others. 2006. The impacts of climate change in coastal marine systems. Ecol. Lett. **9:** 228–241.

Hearn, C. J., and J. L. Largier. 1997. The summer buoyancy dynamics of a shallow Mediterranean estuary and some effects of changing bathymetry: Tomales Bay, California. Estuar. Coast. Shelf Sci. **45:** 497–506.

Kimbro, D. L., and E. D. Grosholz. 2006. Disturbance influences oyster community richness and evenness, but not diversity. Ecology **87:** 2378–2388.

Kimmerer, W. J. 1993. Distribution patterns of zooplankton in Tomales Bay, California. Estuaries **16:** 264–272.

Kirby, M. X. 2004. Fishing down the coast: Historical expansion and collapse of oyster fisheries along continental margins. Proc. Natl. Acad. Sci. USA **101:** 13096–13099.

Largier, J. L. 2003. Considerations in estimating larval dispersal distances from oceanographic data. Ecol. Appl. **13:** S71–S89.

———, C. J. Hearn, and D. B. Chadwick. 1996. Density structures in "low-inflow estuaries," p. 227–241. *In* D. G. Aubrey and C. D. Friederichs [eds.], Coastal and estuarine studies. V. 53. American Geophysical Union.

———, J. T. Hollibaugh, and S. V. Smith. 1997. Seasonally hypersaline estuaries in Mediterranean-climate regions. Estuar. Coast. Shelf Sci. **45:** 789–797.

———, and others. 2006. WEST: A northern California study of the role of wind-driven transport in the productivity of coastal plankton communities. Deep-Sea Res. II **53:** 2833–2849.

Leslie, H. M., E. N. Breck, F. Chan, J. Lubchenco, and B. A. Menge. 2005. Barnacle reproductive hotspots linked to nearshore ocean conditions. Proc. Natl. Acad. Sci. USA **102:** 10534–10539.

Mann, K. H., and J. R. N. Lazier. 2006. Dynamics of marine ecosystems: Biological-physical interactions in the oceans, 3rd ed. Blackwell Publishing.

Menge, B. A. 1992. Community regulation—under what conditions are bottom-up factors important on rocky shores. Ecology **73:** 755–765.

———, and G. M. Branch. 2001. Rocky intertidal communities, p. 221–251. *In* M. D. Bertness, S. D. Gaines, and M. E. Hay [eds.], Marine community ecology. Sinauer Associates.

———, F. Chan, and J. Lubchenco. 2008. Response of a rocky intertidal ecosystem engineer and community dominant to climate change. Ecol. Lett. **11:** 151–162.

———, B. A. Daley, P. A. Wheeler, and P. T. Strub. 1997. Rocky intertidal oceanography: An association between community structure and nearshore phytoplankton concentration. Limnol. Oceanogr. **42:** 57–66.

———, and others. 2003. Coastal oceanography sets the pace of rocky intertidal community dynamics. Proc. Natl. Acad. Sci. USA **100:** 12229–12234, doi:10.1073/pnas.1534875100.

Pinones, A., J. C. Castilla, R. Guinez, and J. L. Largier. 2007. Nearshore surface temperatures in Antofagasta Bay (Chile) and adjacent upwelling centers. Cienc. Mar. **33:** 37–48.

Pitcher, G. C., and G. Nelson. 2006. Characteristics of the surface boundary layer important to the development of red tide on the southern Namaqua shelf of the Benguela upwelling system. Limnol. Oceanogr. **51:** 2660–2674.

Quinn, G. P., and M. J. Keough. 2002. Experimental design and data analysis for biologists. Cambridge Univ. Press.

Sanford, E., and B. A. Menge. 2001. Spatial and temporal variation in barnacle growth in a coastal upwelling system. Mar. Ecol. Prog. Ser. **209:** 143–157.

Smith, S. V., J. T. Hollibaugh, and S. Vink. 1989. Tomales Bay, California—a case for carbon-controlled nitrogen cycling. Limnol. Oceanogr. **34:** 37–52.

Stachowicz, J. J. 2001. Mutualism, facilitation, and the structure of ecological communities. Bioscience **51:** 235–246.

Vander Woude, A. J., J. L. Largier, and R. M. Kudela. 2006. Nearshore retention of upwelled waters north and south of Point Reyes (northern California)—Patterns of surface temperature and chlorophyll observed in CoOP WEST. Deep-Sea Res. II **53:** 2985–2998.

Wilkerson, F. P., A. M. Lassiter, R. C. Dugdale, A. Marchi, and V. E. Hogue. 2006. The phytoplankton bloom response to wind events and upwelled nutrients during the CoOP WEST study. Deep-Sea Res. II **53:** 3023–3048.

Wing, S. R., J. L. Largier, L. W. Botsford, and J. F. Quinn. 1995. Settlement and transport of benthic invertebrates in an intermittent upwelling region. Limnol. Oceanogr. **40:** 316–329.

Associate editor: Christopher M. Finelli

Received: 10 September 2008
Accepted: 02 March 2009
Amended: 01 April 2009